# Risk optimization of RC beam under column loss scenario

Lucas da Rosa Ribeiro[1], André Teófilo Beck[1]

[1]*Dept. of Structural Engineering, University of São Paulo*
*Av Trabalhador São-carlense, 400, 13566-590, São Carlos, SP, Brazil*
*lucasribeiro@usp.br , atbeck@sc.usp.br*

**Abstract.** The sudden column loss of a single supporting element in a RC frame may lead to the disproportionate partial or total structural collapse if its design fails to confine the initial damage through resisting mechanisms. Since uncertainties like material properties and geometrical parameters plays a major role in the behavior of the resisting mechanisms, and consequences are highly significant for such failure events, the risk optimization is a very convenient tool to optimize the balance between economy and safety. This is shown herein by the optimization of a RC beam sub assemblage, considering the beam height, longitudinal steel rebar areas, stirrup cross section area and stirrup spacing as design variables. Failure consequences are included for service limit state, ultimate limit state of confined concrete at snap-through instability, and ultimate limit state of the steel rebars at catenary action stage. A physical and geometrical nonlinear static analysis is employed, in which the samples are submitted to pushdown displacement control over the removed column. Material behavior is represented by an elastoplastic model with isotropic hardening for the steel rebars, and by combination of Mazars μ model with the modified Park-Kent model for the confined concrete. Failure probabilities are evaluated by the Weighted Average Simulation Method, and the Risk optimization is done by the Firefly Algorithm. In order to reduce the computational cost due to the nonlinearities involved and the high number of sample points required, Kriging is used to generate a sufficiently accurate metamodel for the limit states and for the system failure probabilities. It is shown, for the analyzed problem, that the confinement of concrete plays the major role in providing structural safety, since a design that survives the initial stages but fails in the instability stage is sudden, not allowing the occurrence of catenary action.

**Keywords:** catenary action, concrete confinement, progressive collapse, reinforced concrete, risk optimization.

## 1 Introduction

Extraordinary events are known to generate loading conditions able to cause structural collapses, like the gas explosion at the Ronan Point Tower (UK, 1968), the terrorist attack at the World Trade Center (NY, 9/11, 2001), and the earthquake at Wenchuan (China, 2008). When under multiple hazards, the probability of structural collapse $P[C]$ is given as:

$$P[C] = \sum_{H} \sum_{LD} P[C|LD,H]\, P[LD|H]\, P[H] \tag{1}$$

where $P[H]$ is the probability of hazard occurrence; $P[LD|H]$ is the conditional probability of local damage for a given hazard $H$; and $P[C|LD,H]$ is the conditional probability of collapse for a given $LD$ and $H$.

Beck et al. [1] uses this formulation considering the product $P[LD|H]\, P[H]$ as the probability of column loss $P_{CL}$, and combines column loss scenarios with normal loading condition in a single objective function in order to study, for a single design variable $\lambda$, the cost-benefit of considering column loss scenarios for continuous beams, floors, and regular frames via analytic approaches. Aiming to expand this study to usual RC structures, this manuscript uses a similar approach in order to study the cost-benefit of considering a single column loss scenario to the design of a RC beam.

# 2 Formulation and implementation

The RC beam considered herein is based on the multiple RC beam-column subassemblies experimentally studied by Yu e Tan [2]. It has a span of 2.75 m, both ends rigid to rotation, concrete cover of 2 cm, and a cross-section base of 15 cm. The unconfined concrete has $f_{cm}$ = 32 MPa, $E_c$ = 27.2 GPa, $f_{ctm}$ = 3.2 MPa, and $\varepsilon_0$ = 0.002. Other variables, such as the limit strains of elastic stage $\varepsilon_{c0}$ and $\varepsilon_{t0}$, ultimate strain $\varepsilon_{20C}$, effective $f_{cm}$ of the confined concrete, and the parameters of the $\mu$-Model [3] depends on the resulting uniaxial curves from the Modified Park-Kent Model [4], which are dependent of the beam height, and disposal, diameter, and spacing between stirrups. The elastoplastic behavior of the longitudinal steel rebars, is represented by an uniaxial isotropic hardening model, with $E_s$ = 210 GPa, $f_y$ = 500 MPa, $K_s$ = 37 GPa, and $\varepsilon_{su}$ = 0.13. Three legged stirrups with yielding strength of $f_{yt}$ = 500 MPa are considered for the entire beam. All mentioned properties are considered continuous along the beam. Random design variables are the cross section beam height, inferior and superior steel rebar areas, cross section area of the stirrups legs, and spacing between stirrups.

## 2.1 Structural analysis

In order to estimate the probabilities of failure, a metamodel via kriging was employed, which requires the evaluation of a sufficient number of support points by an accurate model of structural analysis. The finite element method based on positions proposed by Coda [5] is used herein, where laminated elements of plane frames are adopted in order to accurately allow the individual representation of concrete and steel. One finite element represents the whole beam, which is discretized in 8 integration points along the element and 21 laminas along its cross-section. Since a sufficient number of laminas is considered, 1 integration point at the transversal direction is considered for each lamina. Stirrups cannot be explicitly considered, but its influence on the ductility of confined concrete is represented by the resulting uniaxial curves from the Modified Park-Kent Model [4], which serves as reference for the automatic calibration of the physical non-linear parameters of the $\mu$-Model [3].

Two structural analysis are done for every beam. Normal Loading Condition (NLC) analysis considers both supports at the beams ends and a uniform load over the beam, and the Column Loss (CL) analysis considers the removal of one support and the beam post-behavior by a control of displacements of 0.5 m at the removed column. The NLC analysis aims to obtain the ultimate uniform load that leads to a maximum mid-span displacement of 5 mm, representing the Service Limit State (SLS). In order to represent the Ultimate Limit State (ULS) after a column loss, the CL analysis aims to obtain the difference between the maximum compressive strain at the confined concrete $|\varepsilon_{c,max}|$ and the ultimate compressive strain for the confined concrete $|\varepsilon_{20C}|$, and also the ultimate displacement at the removed support that leads to the steel rebar failure at catenary action beam stage. In addition, shear failure is neglected due to the beam span $L$ being always greater than 10 times the beam height.

## 2.2 Kriging

Kriging is used to estimate a simplified, but accurate, model of the limit states and of the system failure probabilities in order to allow the realization of the risk optimization, otherwise it would be completely unviable due to the high computational cost required in the structural analysis and estimation of the failure probabilities. The choice of this metamodeling technique is due to its verified high efficiency and robustness for structural reliability problems, besides the fact of having great performance for multi-dimensional analysis [6].

A sufficient number of support points $n_S$ is required in order to make the estimated model accurate relative to the original model. The base of functions chosen to generate the simplified model is a cubic polynomial with all the possible crossed terms. Also, the hyperparameters $\boldsymbol{\theta}$ are considered non-isotropic, being calibrated by the minimization of the maximum likelihood function of Dubourg [7] (eq. (2)) via the Firefly Algorithm.

$$\boldsymbol{\theta} = \arg\min_{\boldsymbol{\theta} \in n\theta} \mathcal{L}(\boldsymbol{\theta}) \; = \sigma^2(\boldsymbol{\theta}) \, |R(\boldsymbol{\theta})|^{1/ns} \tag{2}$$

where $n\theta$ is the number of hyperparameters to be evaluated, $\sigma^2(\boldsymbol{\theta})$ is the metamodel variance, and $R(\boldsymbol{\theta})$ is the matrix containing the correlation between pairs of support points.

### 2.3 Failure probabilities estimation

The $n_{sp}$ sample points obtained by metamodeling of the limit states are used to compose the estimated failure probability $\hat{P}_f$, for the respective failure modes, by the Weighted Average Simulation Method (WASM) proposed by Rashki et al. [8] (eq. (3)). This technique is appropriate for optimization problems involving random design variables since the estimation of $\hat{P}_f$ depends only on the index function $I(x)$ and the weight index $W(x)$ of the $n_{sp}$ sample points. Therefore, changing the mean value of the candidate for optimal design only requires the re-evaluation of the weight index $W(x)$.

$$\hat{P_f} = \frac{\sum_{k=1}^{n_{sp}} I(x_k)\, W(x_k)}{\sum_{k=1}^{n_{sp}} W(x_k)} \tag{3}$$

Since the random design variables are associated with low uncertainties (Table 1), it is required a big number of sample points to accurately estimate the failure probabilities for all the optimal candidates. In addition, since every random design variable has low uncertainty, the difference between the sampling domain and the design domain is small (2 cm for beam height, 0.2E-4 m² for steel rebar areas, 0.5E-5 m² for cross-section area of stirrups, and 1 cm for spacing between stirrups).

Table 1. Uncertainties considered

| Variable | Distribution | Mean ($\mu$) | Standard deviation ($\sigma$) or coefficient of variation ($\delta$) |
|---|---|---|---|
| Beam height ($h$) | Normal | Optimal value searched | 1 cm ($\sigma$) |
| Inferior steel rebar area ($A_{si}$) | Normal | Optimal value searched | 0.05 ($\delta$) |
| Superior steel rebar area ($A_{ss}$) | Normal | Optimal value searched | 0.05 ($\delta$) |
| Stirrups cross section area ($A_{st}$) | Normal | Optimal value searched | 0.05 ($\delta$) |
| Spacing between stirrups ($s_t$) | Normal | Optimal value searched | 0.05 ($\delta$) |
| Intensity of the uniform load for SLS ($q$) | Gumbel | 40 kN/m | 10 kN/m ($\sigma$) |

### 2.4 Risk optimization

The risk optimization problem follows the total expected cost $C_{TE}$ formulation proposed by Beck et al. [1], as shown in eq. (4).

$$C_{TE} = C_M\left[1 + k_{SLS}\, C\, P_f(SLS) + k_{ULS,concr}\, P_f(ULS, concr)P_{LD} + k_{ULS,rebars}\, P_f(ULS, rebars)P_{LD}\right] \tag{4}$$

where $C_M$ is the manufacture cost; $k_{SLS}$, $k_{ULS,concr}$ and $k_{ULS,rebar}$ are the multiplier costs for service limit state, ultimate limit state of concrete and ultimate limit state of the steel rebars, respectively; $P_f(SLS)$, $P_f(ULS, concr)$ and $P_f(ULS, rebars)$ are the failure probabilities for service limit state, ultimate limit state of concrete and ultimate limit state of the steel rebars, respectively; and $P_{LD}$ is the local damage probability representative of the column loss scenario (substituting the $P_{CL}$ from Beck et al.[1]).

The SINAPI database is adopted to estimate $C_M$ in R$, where unencumbered prices for Rio de Janeiro regarding the period of June 2021 are considered. Hence, $C_M$ is composed by cost of formwork, obtainance of concrete, pouring of concrete, obtainance of steel rebars, and placing of steel rebars. Since failure costs are represented by the product of the multipliers $k$ times $C_M$, $k$ is chosen according to the order of magnitude of the failure mode: $k_{SLS}$ = 5 (assuming that SLS leads to loss of usage and equipment), $k_{ULS,concr}$ = 60 and $k_{ULS,rebar}$ = 30. The multiplier for concrete failure is chosen as double of the steel multiplier because concrete fails in the snap-through instability stage in a fragile manner before the occurrence of catenary action.

# 3 Results

The following results were obtained considering 1431 support points in the metamodeling of the limit states obtained via FEM (service limit state, ultimate limit state of confined concrete at snap-through instability, and ultimate limit state of tensioned steel rebar at catenary action); 1500 support points for metamodeling the system failure probabilities; failure probabilities of support points estimated via WASM, considering 3 million sample points which were obtained via metamodel of limit states; firefly algorithm for the risk optimization (40 fireflies, 50 iterations, 10 distinct processes + auxiliary extensive search), calibration of hyperparameters (20 fireflies, 20 iterations, 10 distinct processes + auxiliary extensive search), and calibration of physical non-linear parameters of concrete (50 fireflies and 100 iterations).

Figure 1 indicates the optimal designs for every value of $P_{LD}$, where 10 distinct optimization processes were realized for each.

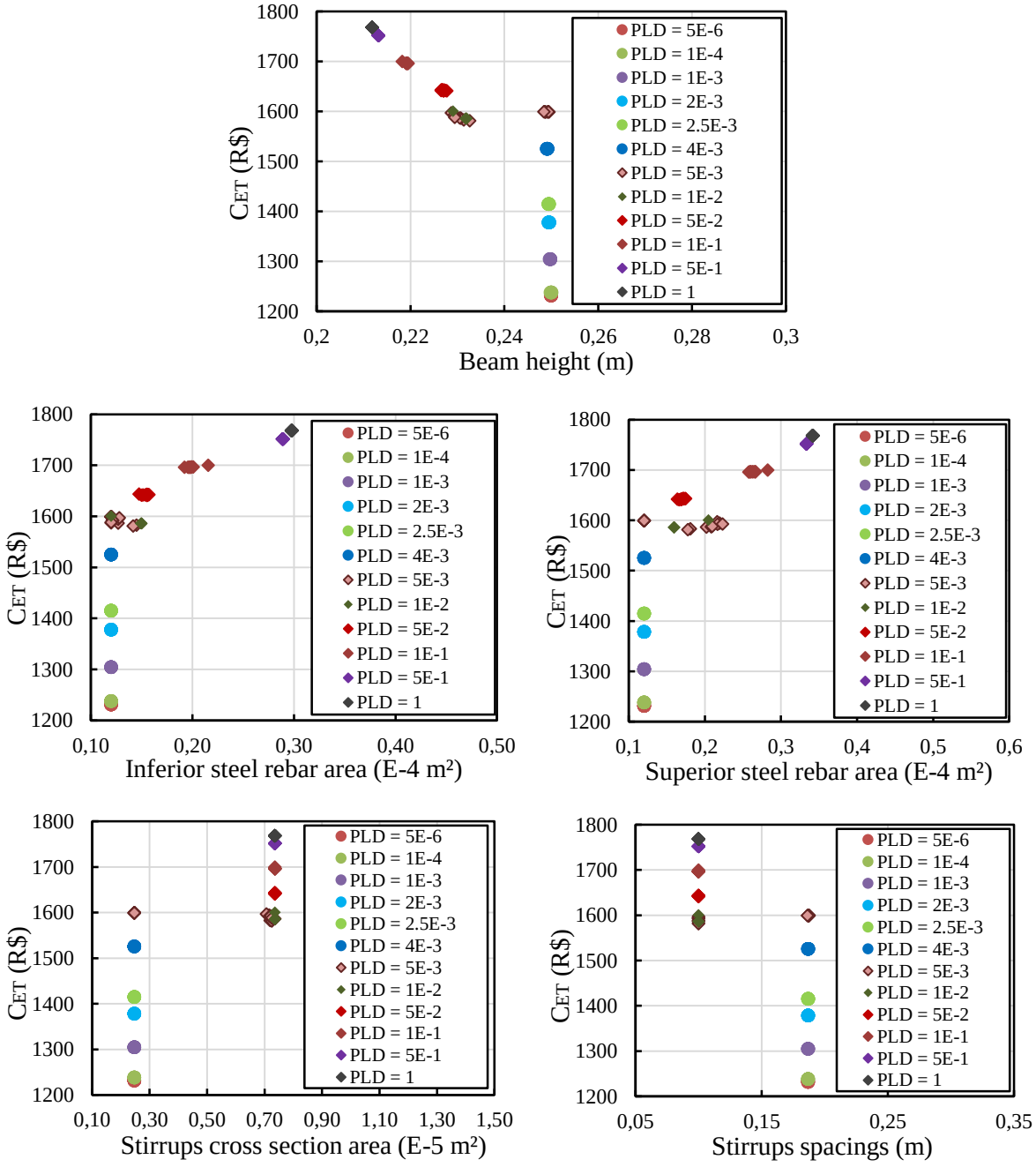


Figure 1. Optimal values for each design variable according to $P_{LD}$

It is noticed that the probability $P_{LD}$= 5E-3 leads to two optimal designs with practically similar $C_{ET}$ which, following the conclusions of Beck et al. [1], suggests to be (approximately) the threshold local damage probability $P_{LD}^{th}$. While the design does not shows positive cost-benefit for considering column loss scenarios, it is shown that the optimal design practically does not change for increasing values of $P_{LD}$. However, the variation of the optimal design increases significantly after $P_{LD}^{th}$, especially for the design variables beam height and steel rebar areas.

The beam height lowers with the increase of $P_{LD}$ due to the fact that, regarding the expected costs of failure, the ultimate limit state of the confined concrete gets more relevant then the service limit state. This happens because a reduced cross section propitiates the confinement of the concrete core, which increases the safety against the ultimate limit state of concrete. In addition, it approximates the superior and inferior steel rebars, which increases the safety against the ultimate limit state of the steel rebars in catenary action. The same is valid for the spacing between the stirrups. Also, it is noticed that the transversal area of the stirrups and its spacing flips from one limit of the design domain to the opposite limit after $P_{LD}^{th}$ is reached. Such behavior is further discussed.

Figure 2 shows the evolution of the optimal reliability indexes $\beta_{SLS}$, $\beta_{ULS,C}$ and $\beta_{ULS,S}$ referred to the service limit state, ultimate limit state of concrete, and ultimate limit state of steel rebars, respectively.

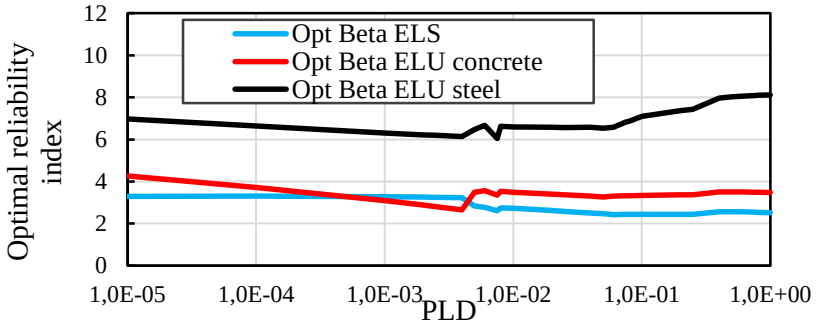


Figure 2. Optimal reliability indexes according to $P_{LD}$

For the problem considered, $P_{LD}^{th}$ is characterized by a transition in the magnitude of the optimal $\beta_{SLS}$ and the optimal $\beta_{ULS,C}$. Besides another transition between the optimal $\beta_{SLS}$ and optimal $\beta_{ULS,C}$ being observed for $P_{LD} \approx$ 7E-4 $< P_{LD}^{th}$, this one does not characterizes another threshold local damage probability because no occurrence of multiple optima with similar $C_{ET}$ was observed. In addition, Fig. 3 shows that $P_{LD}^{th}$ is associated with a flip in the expect costs of failure of service limit state ($C_{EF,SLS}$) and ultimate limit state of concrete ($C_{EF,ULSC}$), which does not happen for $P_{LD}$ = 7E-3.

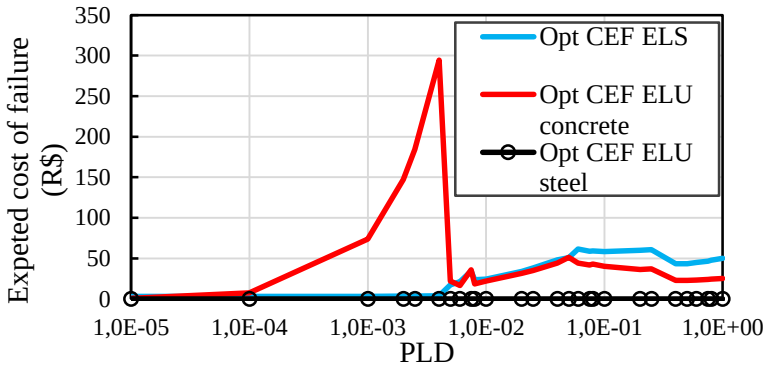


Figure 3. Optimal values for each design variable according to $P_{LD}$

Hence, $P_{LD}^{th}$ is defined herein as the local damage probability after which there is positive cost-benefit in considering column loss scenarios in the design, being characterized by a sudden change in the priority of the considered failure modes. For $P_{LD} < P_{LD}^{th}$, the optimal design allows a $C_{EF,ULS}$ for concrete almost 24% of the beam manufacture cost. However, after $P_{LD}^{th}$ the optimal design changes in order to turn the $C_{EF}$ for SLS higher than the $C_{EF}$ for ULS of concrete. Besides the SLS being allowed to have a higher risk, it is guaranteed a reduced risk for the ULS of concrete.

In order to estimate the behavior of $C_{TE}$ for the design variables involved, the values of 4 of them is fixed equal to the average result of their respective optimal values, and the value of the remaining variable is gradually increased, as shown in Figure 4.

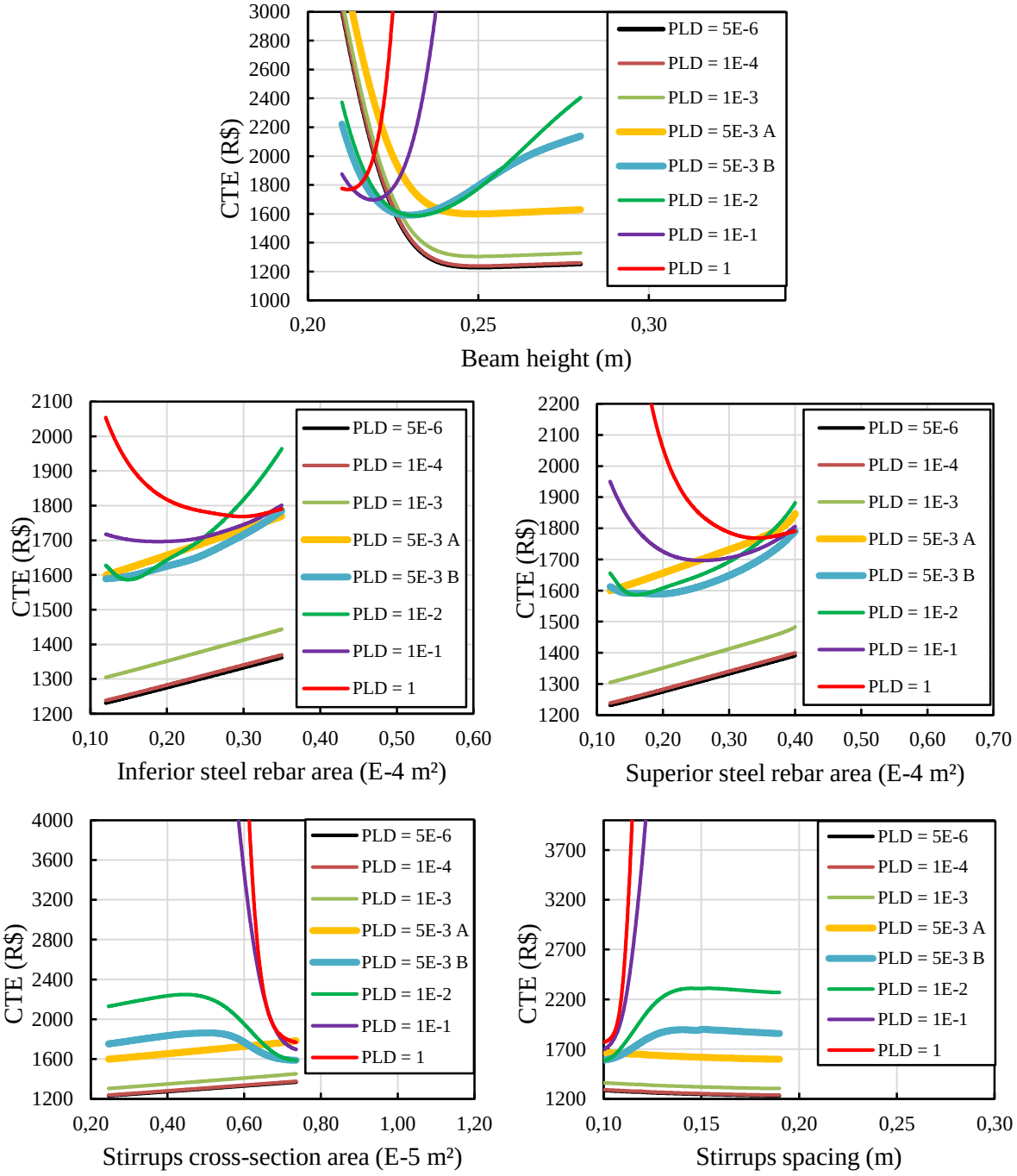


Figure 4. Evolution of $C_{TE}$ by the gradual variance of one design variable at the optimal point

With exception of the beam height variable, all of them shows a linear behavior for $P_{LD} < P_{LD}^{th}$. This reflects the behavior approximately linear of RC beams in service situations. Two curves are shown for $P_{LD}^{th}$, each considering the average value of one of the two verified in Fig. 1. This leads to two distinct minimal values for beam height, cross-section area of stirrups, and spacing between stirrups. However, the difference between the two distinct minimal values is less prominent for the longitudinal steel rebar areas. It is also noticed that the two distinct minimal values for the cross section area and spacing of stirrups coincide with the limits of the design domain, justifying the abrupt flip observed for these variables in Fig. 1 after $P_{LD}^{th}$.

After $P_{LD}^{th}$ there is a gradual reduction in the beam height due to the SLS becoming less relevant than the ULS of the confined concrete at the snap-through instability. Also, there is the gradual increase in the longitudinal steel rebar areas in order to guarantee more safety against both ultimate limit states: concrete at snap-through instability (since more compressive stress is able to be resisted by the steel at this stage, assisting the confined concrete) and steel at catenary action (since larger displacements are allowed for the same ultimate steel strain).

The optimal longitudinal steel rebar areas are not symmetrical for $P_{LD} > P_{LD}^{th}$, since the superior steel rebar area is always slightly larger. As observed in the FEM analysis, this is due to the consideration of the service limit state at the $C_{TE}$. The superior steel rebar area tends to yield before the inferior steel rebar area at the beam's ends for NLC, leading to an increased mid-span displacement after this plastification. Therefore, a larger superior steel rebar is needed in order to efficiently resist the applied load, postpone its yielding, and consequently avoid an increased mid-span deflection. However, if only the column loss scenario is considered, both steel rebar areas results symmetrical.

Also, after $P_{LD}^{th}$ the $C_{TE}$ increases significantly fast for cross section area of stirrups inferior to the optimal and spacing between stirrups superior to the optimum. This reflects the increase in the structural predisposition to the occurrence of concrete failure at the instability stage if the stirrups are placed in a way that reduces the concrete confinement.

# 4 Conclusions

This manuscript shows how the behavior of the optimal design of a RC beam suddenly changes after the consideration of a column loss scenario starts to have a positive cost-benefit. The optimal beam height tends to reduce once SLS shows to be less relevant than the ULS of concrete, showing that an increased confinement level due to a reduced section starts to be preferable than an increased moment of inertia against mid-span deflections. The optimal steel rebar areas tends to increase after $P_{LD}^{th}$ in order to assist the confined concrete at the instability stage, and also allowing larger displacements at the removed support at catenary action. However, since the SLS is always considered, the optimal superior steel rebar area is always greater than the inferior in order to postpone its yielding. Also, the optimal cross section area and spacing between stirrups shows the greatest change after $P_{LD}^{th}$, since the optimization leads to a minimal confinement level due to stirrups when SLS controls the process, but leads to a maximum confinement level due to stirrups as soon as the ULS of concrete starts to control the process.

**Acknowledgements.** Funding of this research project by Brazilian agencies CAPES (Brazilian Higher Education Council), CNPq (Brazilian National Council for Research, grant n. 306373/2016-5), joint FAPESP-ANID (São Paulo State Foundation for Research - Chilean National Agency for Research and Development, grant n. 2019/13080-9) and FAPESP (grant n. 2019/23531-8).

**Authorship statement.** The authors hereby confirm that they are the sole liable persons responsible for the authorship of this work, and that all material that has been herein included as part of the present paper is either the property (and authorship) of the authors, or has the permission of the owners to be included here.

# References

[1] A. T. Beck, L. R. Ribeiro, and M. Valdebenito. Risk-based cost-benefit analysis of frame structures considering progressive collapse under column removal scenarios. *Engineering Structures*, vol. 225, pp. 111295, 2020.

[2] J. Yu and K. H. Tan. Experimental and numerical investigation on progressive collapse resistance of reinforced concrete beam Column sub-assemblies. *Engineering Structures*, vol. 55, pp. 90-106, 2013.

[4] R. Park, M. J. N. Priestley, and W. D. Gill. Ductility of square-confined concrete columns. *Journal of Structural Engineering*, ASCE, vol. 108, n° ST4, pp. 929-950, 1982.

[3] J. Mazars, F. Hamon, and S. Grange. A new 3D damage model for concrete under monotonic, cyclic and dynamic loadings. *Materials and Structures*, vol. 48, pp. 3779-3793, 2015.

[5] H. B. Coda. O método dos elementos finitos posicional: sólidos e estruturas- não linearidade geométrica e dinâmica, 1st ed. São Carlos: EESC-USP, v. 1, 2018.

[6] H. M. Kroetz. Otimização estrutural sob incertezas: métodos e aplicações. Thesis, Universidade de São Paulo, 2019.

[7] V. Dubourg. Adaptive surrogate models for reliability anlysis and reliability-based design optimization. Thesis, Université Blaise Pascal, 2011.

[8] M. Rashki, M. Miri, and M. A. Moghaddam. A new efficient simulation method to approximate the probability of failure and most probable point. *Structural Safety*, vol. 39, pp. 22-29, 2012.